# Process Optimization of Cadmium Adsorption on Blended Bamboo Saw Dust/Rice-Husk from Aqueous Solution Using the Response Surface Methodology

Muhajir Mussa Kwikima[1,2] · Yonas Chebude[1,3] · Beteley Tekola Meshesha[1,4]

## Abstract

Blending two or more feedstocks to enhance the adsorptive capacity of adsorbent materials for pollutant removal in aqueous systems has recently gained more attention. In this article, the adsorptive capability of blended bamboo (*Oxytenanthera abyssinica*) sawdust/rice husk (BSD/RH) at a ratio of 1:1 for the sorption of cadmium ions from aqueous solutions in batch mode was studied. The key process variable parameters; initial $Cd^{2+}$ concentration (20–200 mg/L), initial solution pH (5–9), ionic strength (0.001–0.02 mol/L of $KNO_3$), adsorbent dose (1–3 g), and contact time (15–180 min) were optimized to achieve maximum removal efficiency by employing the Box–Behnken design in response surface methodology. Results showed that; all variable operating parameters were significant in the removal process of $Cd^{2+}$ from the solution by BSD/RH adsorbent, initial $Cd^{2+}$ concentration, and adsorbent dosage being the most significant. The optimum $Cd^{2+}$ removal of 90.56% and 88.97% of predicted and experimental respectively, were obtained at the pH (8.9), ionic strength (0.012 mol/L), contact time (125.93 min), and adsorbent dose (1.99 g). The optimized conditions were later used to study the $Cd^{2+}$ removal efficiency of individual rice husk and bamboo sawdust and found 61.43 and 69.68% respectively. This observation signpost the potential of utilizing the biosorbent derived from blended feedstocks materials on removing heavy metals as cadmium.

**Keywords** Bamboo sawdust/rice husk · Cadmium removal · Optimization · Response surface methodology

## 1 Introduction

Water is considered a vital resource because it is necessary for human livelihood and ecosystem existence. Nevertheless, both natural and anthropogenic influences have been adding up various pollutants to the ground and surface water systems. Heavy metals are among the most serious pollutants added by the aforesaid influences [1].

As a result of the rapid development of industry and hastened urbanization, heavy metal pollution has become a serious environmental hazard, particularly in water bodies [2].

Cadmium is at the top of the list of extremely dangerous heavy metals that pose a serious concern to human health and the environment due to its high toxicity and bioaccumulation potential [3]. It is a well-known and harmful heavy metal in nature that results from natural and anthropogenic activities, primarily textile industries, mining, pesticide, fertilizer in agricultural activity, and wastewater, among other things [4].

It is critical to remove cadmium from wastewater before it is disposed of away. Metal recovery from aqueous media is a difficult process that requires a range of techniques and separation principles [5]. Filtration, sedimentation, electrochemical processes, membrane processes, reverse osmosis, adsorption, coagulation, sono-chemical separation, and other methods have been used to remove metals from wastewater and aqueous solutions [6–11], with "limited metal removal, high chemical, energy, and high-tech equipment required, production of toxic sludge, or end-products that require

✉ Muhajir Mussa Kwikima
muhajirmussa@gmail.com

1 African Centre of Excellence for Water Management, College of Natural and Computational Sciences, Addis Ababa University, P.O. Box 1176, Addis Ababa, Ethiopia

2 Department of Environmental Engineering and Management, College of Earth Sciences and Engineering, The University of Dodoma, P.O. Box 11090, Dodoma, Tanzania

3 Department of Chemistry, Addis Ababa University, Addis Ababa, Ethiopia

4 School of Chemical and Bio Engineering, Addis Ababa University, Addis Ababa, Ethiopia

disposal" being mentioned as drawbacks to many of the methods. Adsorption has been recognized as one of the most frequent strategies due to its simplicity in operation, ease of recovery, high efficiency, cost-effectiveness, and renewability. Nonetheless, due to the multi-faceted nature of the action, selecting an ultimate adsorbent remains difficult. For this purpose, an appropriate adsorbent material should have a high surface area, high removal efficiency, and adsorption capacity, as well as mechanical stability [12].

Agricultural waste products have been shown to be eco-friendly and to have potential biosorption capacity among the various adsorbent materials available. "The advantages of employing agricultural wastes as biosorbents compared to conventional wastewater treatment systems are (1) reduced sludge generation, (2) recycling and renewability, (3) local availability, (4) high efficiency, and (5) low cost," according to Bhatnagar et al. [13]. A number of chemical groups such as carboxyl, carbonyl, hydroxyl, and amine groups in their macromolecules (hemicellulose, lignin, proteins, humic substances, and cellulose) have been proven to be found in Plant-derived biomass [14]. These chemical groups have crucial adsorptive properties mostly for ion- exchange or other interaction mechanisms. Varala et al. [14] listed the types of functional groups present on the biomass surface, and metal-ion types as the major influences of the biosorption mechanism include. Available literature reveals the potentials of abundant agricultural waste materials, including wheat husk and bran, sawdust of several woody plants, the bark of the trees, rice husk and bran, ground-nut and coconut shells, bamboo sawdust, sugarcane bagasse, orange peels, and many more [15–18]. Enhancing further adsorption improvement to these adsorbent materials, different physical and chemical modifications such as enhancement of binding groups, elimination of inhibiting groups, pyrolysis, graft polymerization, etc., have been adopted [2]. Contrary; many of these enhancement approaches such as graft polymerization and elimination of inhibiting groups are associated with operation high cost and others like chemical adsorbent surface activation necessitate further treatment of effluents since they employ some bases, mineral and organic acids, and some strong oxidizing agents. However, recently it has been revealed that the application of blended feedstocks of these agricultural wastes can as well enhance removal efficiency with minimal operational costs as well as reduced effluent treatment requirements [19–26]. Although the focus has been mostly on the biochars rather than raw/unmodified agricultural wastes feedstocks. Blending more than one feedstock to make a biosorbent has been proven to have a synergetic effect on the overall removal of pollutants from an aqueous system [23, 24].

Various countries around the world cultivate rice as a food crop, with approximately 700 million tonnes annual harvest. The rice milling process is associated with the production of a huge amount of residual rice husk approximating nearly 23 wt% of the rice [27]. Utilizing rice husk as a biosorbent will further improve the value chain of rice production since it has low nutritional value and high ash content where currently no economical use of it is practiced.

The greatest bamboo reserve in Africa is in Ethiopia, covering more than 1 million hectares of land [28]. Due to its fastest-growing and high-yielding characteristics, its uses have been increasing rapidly in a country as a substitute for slow-growing woody plants as a building material and other purposes [29]. Its processing mainly employs rudimentary technologies mostly low end- handcrafts [30] that are associated with significant production of wastes including sawdust among others, which currently has no further economical use.

Furthermore; the two feedstocks [bamboo sawdust (BS) and rice husk (RH)] are effective biosorbents due to their low moisture, high carbon, and lignocellulose contents [25, 31–34]. These two aforesaid reasons influenced the selection of the biosorbent materials for the study. The chemical makeup of rice husk and bamboo sawdust (*Oxytenanthera abyssinica*) employed in this study is summarized in Table 1.

As a result, the goal of this work was to determine the $Cd^{2+}$ removal effectiveness of an unmodified agricultural waste biosorbent generated from a 1:1 blend of rice husk and bamboo sawdust in an aqueous solution. Response surface methodology (RSM) was used to optimize influencing parameters (pH, contact time, ionic strength, adsorbent dosage, and initial solute concentration). Aktar [35] reported the chosen influencing parameters on this study as the major factors affecting the biosorption process and hence adopted for optimization.

Changing one influencing factor while keeping the others constant at a certain set of conditions has been used to optimize influencing factors. This technique necessitates a large number of runs and is time-consuming, which most likely results in poor optimization due to the omission of some interactions [38]. A RSM technique can easily remedy this gap. D-optimal design (DOP) [38], factorial design (FD) [39], central composite design (CCD) [40], and Box–Behnken design (BBD) [41], are some of the designs used in the process. Despite the fact that they both provide

**Table 1** Some chemical compositions of rice husk and bamboo sawdust (*Oxytenanthera abyssinica*) that was used in this research work

| | Cellulose (%) | Lignin (%) | Hemicellulose (%) | References |
|---|---|---|---|---|
| Rice husk | 50 | 25–30 | 15–25 | [36] |
| Bamboo sawdust (*Oxytenanthera abyssinica*) | 52 | 22.47 | 16.90 | [37] |

enough information, the first three designs are less economical than the last due to the increased number of tests required. Additionally, "The combinations in which all factors are at their highest or lowest levels at the same time, the BBD does not hold. This is important in dodging experiments performed under extreme conditions that may cause insufficient results" [42], hence adopted to perform the task.

To the knowledge of the authors, no similar previous work has been reported on the internet accessed platforms on the adsorption process of rice-husk/bamboo sawdust for cadmium biosorption.

# 2 Materials and Methods

## 2.1 Preparation of 1:1 Blended Bamboo Sawdust/ Rice Husk Biosorbent Material

The experiment was carried out in Analytical Chemistry Laboratory, at the College of Natural and Computational Sciences of the University of Addis Ababa where the needed chemicals and other apparatus were purchased from reliable dealers in and out of Ethiopia. The chemicals and solvents used were all reagent grade. Rice husks were collected from rice processing mills from the city of Woreta, Ethiopia; while the lowland bamboo (*Oxytenanthera abyssinica*) was purchased from Gumuz region, Ethiopia. Rice husk and bamboo sawdust were ground and the powder mixed thoroughly at a ratio of 1:1 to homogenize the mixer in equal proportion (Bamboo was cut into small pieces and crushed by crusher before grinding). For the study of the $Cd^{2+}$ removal efficiency of an individual feedstock, a portion of these powders was kept unmixed. Afterward; the mixture was sieved and washed with de-ionized water to remove some impurities, later sun-dried for a week, and finally kept on a dry polythene bag ready to be used for the study.

## 2.2 Physicochemical Properties Analysis

In this study, the properties analyzed on the adsorbent material were the point of zero charges and BET surface area. The point of zero charges of the adsorbent was measured by pH drift-method using a Eutech instruments PH 700 series, pH meter (the pH values were adjusted to an initial pH value of 2, 4, 6, and 8 using 0.1 M NaOH and 0.1 M HCl solution). Where 0.1 M NaCl was used as electrolyte solution at 0.1 g dose. The specific surface area ($S_{BET}$) was examined by the SA-9600 Series Surface Area Analyzer (Horiba Instruments, Inc). Functional groups were also measured on Spectrum 65 FT-IR (PerkinElmer) in the range 4000–400 $cm^{-1}$ (resolution: 4 $cm^{-1}$, number of scans: 4) using KBr pellets.

## 2.3 Cadmium Adsorption Experiments

A 1000 mg/L $Cd^{2+}$ stock solution was prepared with hydrate cadmium chloride ($CdCl_2 \cdot H_2O$) by dissolving 17.9 g of hydrated salt into a liter of de-ionized water in a 1 L volumetric flask. Similarly, 1 M of $KNO_3$ stock solution was prepared by dissolving 10.11 g of $KNO_3$ in a liter of de-ionized water in the 1 L volumetric flask. For each batch, different volumes of $Cd^{2+}$ and $KNO_3$ were diluted in a 25 mL volumetric flask to make three levels of solute concentrations and ionic strength using the dilution equation. 25 mL as the final volume of each batch experiment of the metal and $KNO_3$ mixture was then poured into a 150 mL Erlenmeyer flask. The pH of the mixture was adjusted using 0.1 M HCl and 0.1 M NaOH after which the adsorbent at different doses was added and the mixture was shaken with a mechanical shaker at 200 rpm, 25 °C temperature, and at different durations of time. The fixed parameters were the adsorbent dose, pH, and Ionic strength as given in Table 2 (levels of these parameters were decided after several pilot experiments guided by available relevant literature). After adsorption, the samples were centrifuged at 3600 rpm for 20 min and then filtered using 0.45 μm Whatman filter paper. The residual concentrations of Cd(II) in the supernatant solutions after dilution were measured using the flame atomic absorption spectrophotometer (ZEEnit 700 P, Analytik jena) using US EPA method 7000B. Measurement of pH was performed using a Eutech instruments PH 700 pH meter. The %removal was calculated using Eq. 1 and the adsorbent adsorption capacity was calculated using Eq. 2.

$$R = \frac{C_i - C_t}{C_i} \times 100, \qquad (1)$$

where R is the removal efficiency (%) of the Cd(II), $C_i$ and $C_t$ are the initial and residual concentrations of Cd(II) (mg $L^{-1}$), respectively.

$$C = \frac{(C_i - C_f)}{M} v, \qquad (2)$$

where C is Cd(II) adsorption capacity of adsorbent (mg/g), $C_i$ and $C_f$ are the initial and residual concentrations of Cd(II)

**Table 2** Coding of experimental factors and levels

| Factor | Variables | Coded variables levels | | |
|---|---|---|---|---|
| | | −1 | 0 | +1 |
| A | pH | 5 | 7 | 9 |
| B | Initial $Cd^{2+}$ concentration (mg/L) | 20 | 110 | 200 |
| C | Ionic strength (mol/L) | 0.001 | 0.0105 | 0.02 |
| D | Adsorbent dosage (g) | 1 | 2 | 3 |
| E | Contact time (min) | 15 | 97.5 | 180 |

(mg L$^{-1}$), respectively, $v$ is the volume of the solution (L) and $M$ is the mass of adsorbent (g).

### 2.3.1 Design of Experiments

Box–Behnken design of RSM was employed to study the influence of initial solute concentration, pH, ionic strength, contact time, and adsorbent dose on the adsorption of Cd$^{2+}$ into the adsorbent. Design Expert 11.1.0.1 including ANOVA and regression to obtain the interaction between the process variables to the response was used to model the result and to generate the runs of the experiment. To present and explain the interactions between variables on the Cd$^{2+}$ removal effect, the plots of two-dimensional and contour were used. Additionally, three-dimensional curves of the response surfaces were also developed.

Response surface methodology "is a collection of mathematical and statistical tools used for designing experiments, modeling processes, studying the effects of independent operational parameters and their interactions, and determining the optimal values of those parameters to achieve an intended result" [43]. The independent variables were coded according to Eq. 3:

$$X_i = \frac{X_I - X_0}{\Delta X},\qquad(3)$$

$X_i$ is the dimensionless coded value of the of $i$th variable, $X_0$ is the value of the variable at the center while $\Delta X$ is the step change. Each of the parameters was coded at three levels of +1, 0, and −1 being the low, center, and high levels respectively. Table 2 shows the experimental design protocol with each independent variable [44].

The empirical second-order polynomial model used to fit the experimental data to obtain the model terms is given as Eq. 4 below as proposed by [45].

$$Y = b_0 + \sum b_{ii}X_i + \sum b_{ii}X_i^2 + \sum b_{ij}X_iX_j\qquad(4)$$

where, $Y$ is the response variables (Cd$^{2+}$ reduction) and $b_0$, $b_i$, $b_{ii}$, and $b_{ij}$ are constant coefficients of intercept, linear, quadratic, and interactive terms, respectively and $X_i$ and $X_j$ represent the five independent variables (pH, initial concentration, ionic strength, adsorbent dosage and contact time).

A total number of 46 batch adsorption experiments were carried out with six replicates at the central points.

## 3 Results and Discussion

As stated in Table 2, the actual values of process variables and their variation limits were determined based on values derived from accessible literature and exploratory experiments. Table 3 shows the actual and expected

Cd$^{2+}$ percentage removal efficiency as well as adsorption capacity by adsorption utilizing BSD/RH adsorbent for various combinations of influencing parameters. The Cd$^{2+}$ concentration in the solution was effectively decreased by the BSD/RH adsorbent material. The percentage removal ranged from 29.5 to 99.9%. As the most suited polynomial regression equation, the quadratic model was suggested. "The model selection is by the sequential model sum of squares which is based on the polynomial's highest order where the model is aliased and the additional significant terms" [44].

### 3.1 Physicochemical Properties Analysis

The point of zero charges (pHZc) of the BSD/RS was found to be around neutral (6.6); this implies that the surface of the adsorbent has a net positive charge. The SBET surface area analysis gave the value of 0 showing that our adsorbent has an insignificant pore.

#### 3.1.1 Fourier Transform Infrared Spectroscopic (FTIR) Analysis

The Fourier transforms infrared (FTIR) spectroscopy provides some information on the accessible functional groups that operate as the contaminant's primary binding site. Agricultural waste biosorbents contain functional groups such as phosphodiester, carbonyl, sulfhydryl, carboxyl, hydroxyl, amine, imine, imidazole, amide, phenolic, phosphate, thioether, and sulfonate [12].

The FTIR spectra can be utilized to examine the vibration frequency changes for different functional groups in the adsorbent [46]. Figure 1 shows the FTIR spectroscopy of BSD/RH before and after Cd(II) adsorption. The following bands were visible in the FTIR spectra of BSD/RH prior to adsorption as presented by the lower plot in Fig. 1: the broad peak at 3382 cm$^{-1}$ indicates the presence of free and hydrogen-bonded −OH (hydroxyl), Si–OH (silanol), and −NH$_2$ (amino) groups, as well as 2919 and 2851 cm$^{-1}$ (C–H in aliphatic), 1743 cm$^{-1}$ (C=O), 1643 cm$^{-1}$ (C=C), 1518 cm$^{-1}$ (C–C in aromatics), 1375 and 1247 cm$^{-1}$ (O–H), and 1045 cm$^{-1}$ (C–O of alcohol).

The intensity and position of peaks in the FTIR spectra following Cd(II) adsorption show some major modifications. The upper plot in Fig. 1, shows the almost complete disappearance of all peak bands which indicates the complete involvement of the functional groups in the adsorption process. Interactions with amines, silanol, hydroxyl, carboxylic, amino, and acid groups have been linked to Cd(II) removal [44].

**Table 3** The Box–Behnken design (BBD) shows the actual and predicted $Cd^{2+}$ removal as well as the adsorption capacity of adsorbent at different combinations of influencing parameters by adsorption using BSD/RH adsorbent

| Run | pH | Cd conc (mg/L) | Ionic strength (mol/L) | Time (min) | Dosage (g) | Actual value (%) | Predicted value (%) | Adsorption capacity (mg/g) |
|---|---|---|---|---|---|---|---|---|
| 1 | 7 | 110 | 0.0105 | 15 | 1 | 58.4 | 62.35 | 64.24 |
| 2 | 7 | 110 | 0.02 | 97.5 | 3 | 98.88 | 103.59 | 36.26 |
| 3 | 7 | 20 | 0.0105 | 15 | 2 | 89.88 | 92.9 | 8.99 |
| 4 | 7 | 110 | 0.0105 | 97.5 | 2 | 86.01 | 91.05 | 47.31 |
| 5 | 7 | 110 | 0.001 | 97.5 | 3 | 90.92 | 89 | 33.34 |
| 6 | 7 | 200 | 0.0105 | 180 | 2 | 94.8 | 97.62 | 94.80 |
| 7 | 7 | 20 | 0.0105 | 97.5 | 1 | 93.24 | 92.09 | 18.65 |
| 8 | 7 | 110 | 0.0105 | 97.5 | 2 | 91.2 | 91.05 | 50.16 |
| 9 | 9 | 20 | 0.0105 | 97.5 | 2 | 96.91 | 95.89 | 9.69 |
| 10 | 7 | 110 | 0.02 | 97.5 | 1 | 51.78 | 54.61 | 56.96 |
| 11 | 9 | 110 | 0.001 | 97.5 | 2 | 94.08 | 99.22 | 51.74 |
| 12 | 7 | 20 | 0.0105 | 97.5 | 3 | 88.27 | 84.76 | 5.88 |
| 13 | 7 | 110 | 0.001 | 15 | 2 | 85.29 | 89.33 | 46.91 |
| 14 | 5 | 110 | 0.0105 | 97.5 | 3 | 97.04 | 97.12 | 35.58 |
| 15 | 9 | 110 | 0.0105 | 180 | 2 | 99.86 | 100.06 | 54.92 |
| 16 | 9 | 110 | 0.0105 | 97.5 | 1 | 79.73 | 77.24 | 87.70 |
| 17 | 7 | 110 | 0.0105 | 97.5 | 2 | 92.3 | 91.05 | 50.77 |
| 18 | 7 | 20 | 0.001 | 97.5 | 2 | 99.92 | 97.21 | 9.99 |
| 19 | 5 | 110 | 0.001 | 97.5 | 2 | 99.7 | 100.28 | 54.84 |
| 20 | 7 | 110 | 0.02 | 15 | 2 | 81.67 | 83.37 | 44.92 |
| 21 | 9 | 110 | 0.0105 | 97.5 | 3 | 99.49 | 102.92 | 36.48 |
| 22 | 7 | 110 | 0.0105 | 180 | 3 | 99.98 | 95.91 | 36.66 |
| 23 | 9 | 110 | 0.02 | 97.5 | 2 | 95.14 | 95.75 | 52.33 |
| 24 | 7 | 110 | 0.001 | 97.5 | 1 | 92.03 | 88.23 | 101.23 |
| 25 | 9 | 200 | 0.0105 | 97.5 | 2 | 83.81 | 82.91 | 83.81 |
| 26 | 7 | 200 | 0.0105 | 180 | 2 | 79.61 | 76.29 | 79.61 |
| 27 | 5 | 200 | 0.0105 | 97.5 | 2 | 60.48 | 65.61 | 60.48 |
| 28 | 5 | 110 | 0.02 | 97.5 | 2 | 88.67 | 84.72 | 48.77 |
| 29 | 7 | 20 | 0.02 | 97.5 | 2 | 96.92 | 94.46 | 9.69 |
| 30 | 7 | 110 | 0.0105 | 15 | 3 | 97.03 | 95.53 | 35.58 |
| 31 | 7 | 110 | 0.001 | 180 | 2 | 99.95 | 101.57 | 54.97 |
| 32 | 5 | 110 | 0.0105 | 15 | 2 | 89.48 | 86.38 | 49.21 |
| 33 | 7 | 200 | 0.0105 | 97.5 | 3 | 88.9 | 91.67 | 59.27 |
| 34 | 5 | 110 | 0.0105 | 97.5 | 1 | 78.89 | 73.06 | 86.78 |
| 35 | 7 | 200 | 0.02 | 97.5 | 2 | 65.12 | 62.4 | 65.12 |
| 36 | 5 | 110 | 0.0105 | 180 | 2 | 95.39 | 97.47 | 52.46 |
| 37 | 7 | 200 | 0.001 | 97.5 | 2 | 81.64 | 78.68 | 81.64 |
| 38 | 5 | 20 | 0.0105 | 97.5 | 2 | 98.21 | 103.22 | 9.82 |
| 39 | 9 | 110 | 0.0105 | 15 | 2 | 98.75 | 93.77 | 54.31 |
| 40 | 7 | 110 | 0.0105 | 97.5 | 2 | 91.2 | 91.05 | 50.16 |
| 41 | 7 | 110 | 0.02 | 180 | 2 | 89.23 | 88.51 | 49.08 |
| 42 | 7 | 110 | 0.0105 | 97.5 | 2 | 96.4 | 91.05 | 53.02 |
| 43 | 7 | 200 | 0.0105 | 15 | 2 | 66.76 | 63.64 | 66.76 |
| 44 | 7 | 200 | 0.0105 | 97.5 | 1 | 29.47 | 34.59 | 58.94 |
| 45 | 7 | 110 | 0.0105 | 180 | 1 | 77.98 | 79.35 | 85.78 |
| 46 | 7 | 110 | 0.0105 | 97.5 | 2 | 89.2 | 91.05 | 49.06 |

**Fig. 1** FTIR spectra of BSD/
RH before Cd and after Cd(II)
adsorption
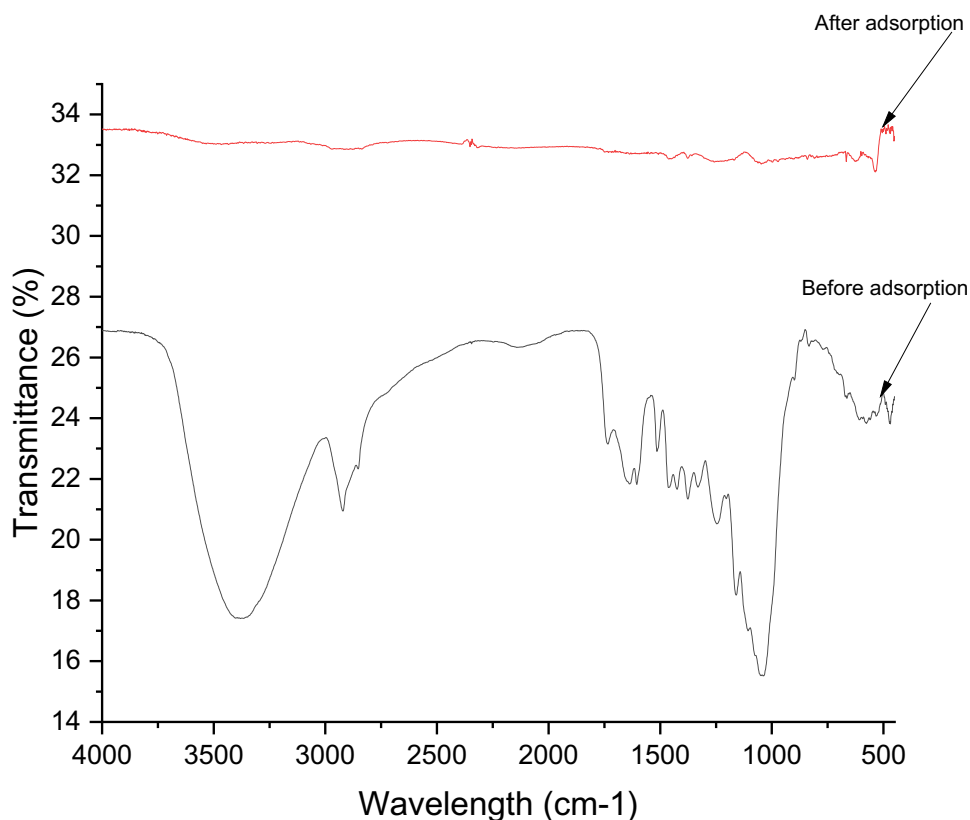


## 3.2 *Adsorption of Cd$^{2+}$ onto BSD/RH Adsorbent*

### 3.2.1 Statistical Analysis

Hill and Hunter [47] states that there are four main phases to implementing RSM with BBD for optimization. "(1) Create and carry out a statistical experimental strategy based on the independent variables. (2) Based on the replies of the experimental results, propose a mathematical model and elaborate the conclusion of the analysis of variance. (3) Diagnostic plots are used to check the model's correctness. (4) Conduct response analysis and anticipate the model's optimal circumstances, as well as verifying the model through an experiment."

### 3.2.2 Model Fitting and Analysis of Variance (ANOVA), Quadratic Model Equations, and Selected Model Diagnostic Test

To examine the logic of the model prediction for BSD/RH Cd$^{2+}$ adsorption, the important findings after analysis of variance are given in Table 4 and regression of the data set disclosed in Table 3. The model coefficients for constant terms, quadratic effects, cubic effects, and interaction effects were all assessed in this study. The low p value of 0.0001

and big F value of 24.36 in the BSD/RH Cd$^{2+}$ adsorption setup [48] indicate that at least one of the variables in each model has a substantial effect on the response.

The lack of fit p value of 0.2836 beings $\geq 0.05$ made lack of fit not significant for the experimental setups [49]. At the same time, its sum of squares (SS) was found to be > 400, this further explains the insignificant lack of fit in the model. As seen from Table 4, the initial pH (A), and initial Cd$^{2+}$ concentration (B), ionic strength (C), contact time (D), and adsorbent dosage (E) are significant to the model, where the most significant parameters were initial Cd$^{2+}$ concentration (B) and adsorbent dosage (E) both with a sum of squares of > 2000, followed by ionic strength (C) then contact time (D) with SS of > 300 and last was pH (A) with SS of 99.55.

For the case of interaction between parameters, the most significant was between initial concentration and adsorbent dosage (BE) with SS of > 1000, contact time and adsorbent dosage (CE) having the SS of > 500 as well as the interaction between themselves initial Cd$^{2+}$ concentration (B$^2$) and adsorbent dosage (E$^2$) where both of these interactions were having SS of > 500 and > 400 respectively. The interaction between pH and initial Cd$^{2+}$ concentration (AB) and that between pH itself (A$^2$) were also significant with the SS value > 100.

**Table 4** ANOVA and regression results for the response surface quadratic model for cadmium removal efficiency by BSD/RH adsorption

| Source | Sum of squares | df | Mean square | F value | p value | |
|---|---|---|---|---|---|---|
| Model | 9117.60 | 20 | 455.88 | 24.36 | <0.0001 | Significant |
| A—PH | 99.55 | 1 | 99.55 | 5.32 | 0.0296 | |
| B—initial concentration | 2559.35 | 1 | 2559.35 | 136.78 | <0.0001 | |
| C—ionic strength | 362.14 | 1 | 362.14 | 19.35 | 0.0002 | |
| D—contact time | 302.24 | 1 | 302.24 | 16.15 | 0.0005 | |
| E—adsorbent dosage | 2474.81 | 1 | 2474.81 | 132.26 | <0.0001 | |
| AB | 151.66 | 1 | 151.66 | 8.11 | 0.0087 | |
| AC | 36.54 | 1 | 36.54 | 1.95 | 0.1746 | |
| AD | 5.76 | 1 | 5.76 | 0.3078 | 0.5839 | |
| AE | 0.6480 | 1 | 0.6480 | 0.0346 | 0.8539 | |
| BC | 45.70 | 1 | 45.70 | 2.44 | 0.1307 | |
| BD | 15.72 | 1 | 15.72 | 0.8402 | 0.3681 | |
| BE | 1036.84 | 1 | 1036.84 | 55.41 | <0.0001 | |
| CD | 12.60 | 1 | 12.60 | 0.6735 | 0.4196 | |
| CE | 581.05 | 1 | 581.05 | 31.05 | <0.0001 | |
| DE | 69.14 | 1 | 69.14 | 3.70 | 0.0660 | |
| $A^2$ | 128.21 | 1 | 128.21 | 6.85 | 0.0148 | |
| $B^2$ | 555.00 | 1 | 555.00 | 29.66 | <0.0001 | |
| $C^2$ | 0.1032 | 1 | 0.1032 | 0.0055 | 0.9414 | |
| $D^2$ | 1.88 | 1 | 1.88 | 0.1007 | 0.7537 | |
| $E^2$ | 465.13 | 1 | 465.13 | 24.86 | <0.0001 | |
| Residual | 467.79 | 25 | 18.71 | | | |
| Lack of fit | 408.73 | 20 | 20.44 | 1.73 | 0.2836 | Not significant |
| Pure error | 59.05 | 5 | 11.81 | | | |
| Cor total | 9585.38 | 45 | | | | |

$R^2 = 0.9512$; adjusted $R^2 = 0.8206$; predicted $R^2 = 0.8206$; adequate precision $= 23.6081$

## 3.3 Ultimate Equation Based on Actual Factors

The below second-order polynomial equation express an empirical relationship between $Cd^{2+}$ % removal efficiency and the variables in terms of actual factors:

$$\% \text{ Removal efficiency} = 166.387 - 17.2947\,\text{pH} + -0.505694\,conc - 3521.35\,is + 0.212099\,t$$
$$+ 12.1442\,dose + 0.0342083\,\text{pH} \times conc + 0.178889\,conc \times dose$$
$$+ 1268.68\,is \times dose + 0.958229\,\text{pH}^2 - 0.000984516\,conc^2 - 7.30042\,dose^2,$$

where *is*, *conc*, *t*, and *dose* stands for the initials of the process variables ionic strength, initial concentration, contact time, and adsorbent dose respectively. The regression coefficient $R^2$ of 0.9512 demonstrates the model's applicability in predicting response in experimental data [49]. The adequate precision of 23.6 also denotes a reasonable and satisfactory signal-to-noise ratio. The modified $R^2$ of 0.9122 is lower than the $R^2$ value, implying that "adding a new number of factors to the model in an attempt to modify it could improve nothing" [48]. Furthermore, the difference of less than 0.2 between the predicted $R^2$ (0.8206) and the adjusted

$R^2$ (0.9122) is in reasonable agreement. The measured $R^2$ values show that the regression models well explained the BSD/RH adsorption process. Hence, the model developed in this study was considered to be satisfactory for predicting $Cd^{2+}$ removal efficiency.

The output can be determined with the premise that both of the models were adequate because the points in the plot form a fairly straight line. Figure 2 displays the normal probability plot of residuals. There should be no series of increasing or decreasing points patterns, such as increasing residuals with increasing fits and a high proportion of positive or negative residuals, for a model to be dependable in the event of actual residual against fit plot [48].

Figure 3 shows an alignment between residuals and expected $Cd^{2+}$ removal, which supports the data provided in Table 4. The close agreement between the actual and
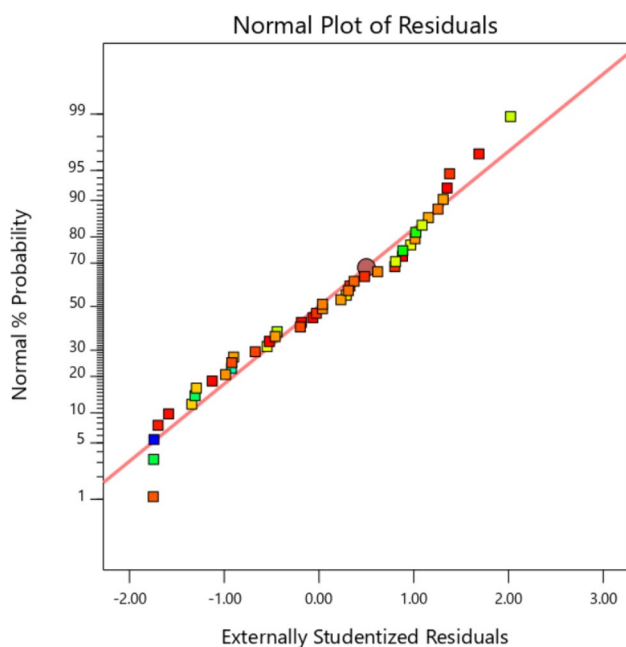
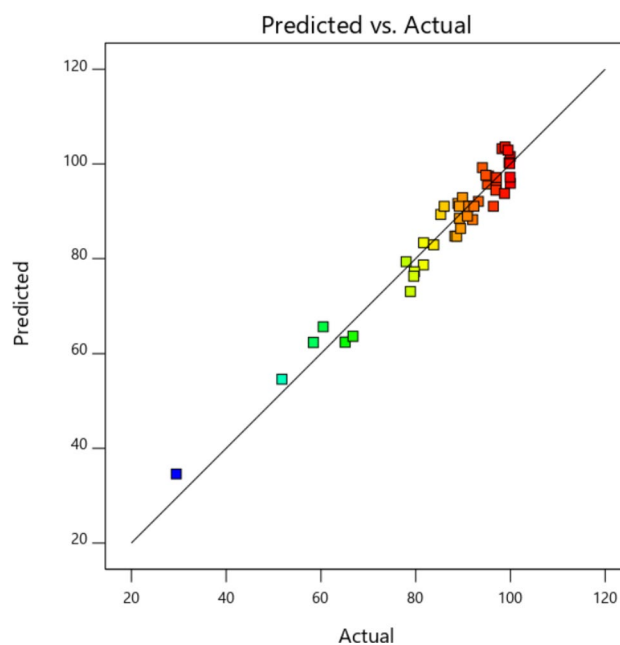Fig. 2 Normal probability plots BSD/RH adsorption process



Fig. 4 Plots for predicted against actual results for $Cd^{2+}$ removal by BSD/RH adsorption process
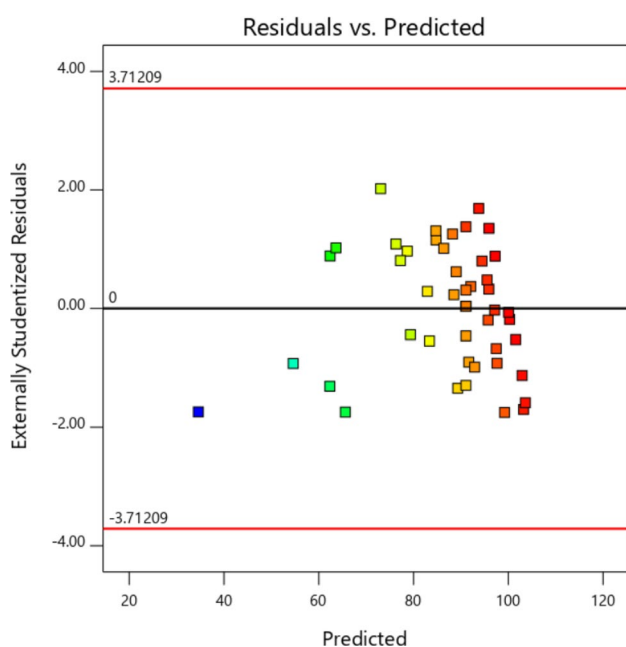


Fig. 3 Residual vs predicted plots for $Cd^{2+}$ removal by BSD/RH adsorption process

anticipated results is further evidenced by the predicted and actual plots in Fig. 4, implying that the model could accurately predict within the range of influencing parameters. As a result, it can be determined that the model established in this work, which correlates $Cd^{2+}$ removal with process factors, is good enough to be adapted to describe the BSD/RH adsorption process' experimental data.

## 3.4 Effect of Individual Operating Parameters

The plots in Fig. 5 indicate the effect of specific operating parameters; pH, ionic strength, treatment time, initial $Cd^{2+}$ concentration, and adsorbent dosage, which were all investigated in this work. The parameters were calculated as a function of the amount of $Cd^{2+}$ removed from the equation. These variables are recognized to be important in adsorption system operation [14, 44].

### 3.4.1 Influence of pH

It can be seen from the plots that when the pH rises, the percentage of $Cd^{2+}$ removed by BSD/RH rises as well. The alkaline pH rose from > 7 to 9 in Fig. 5a, indicating a considerable rise. In general, when cationic metals are removed through biosorption, the pH of the solution rises, while anionic metals fall. The biosorbent will have a positive total surface charge at lower pH. $H^+$ ions effectively compete with metal cations, lowering biosorption capability. The biosorbent surface becomes increasingly negatively charged as pH values rise, favoring the uptake of metal ions due to electrostatic interaction The biosorption process comes to a halt at a very high pH, and the precipitation of hydroxide begins [12].
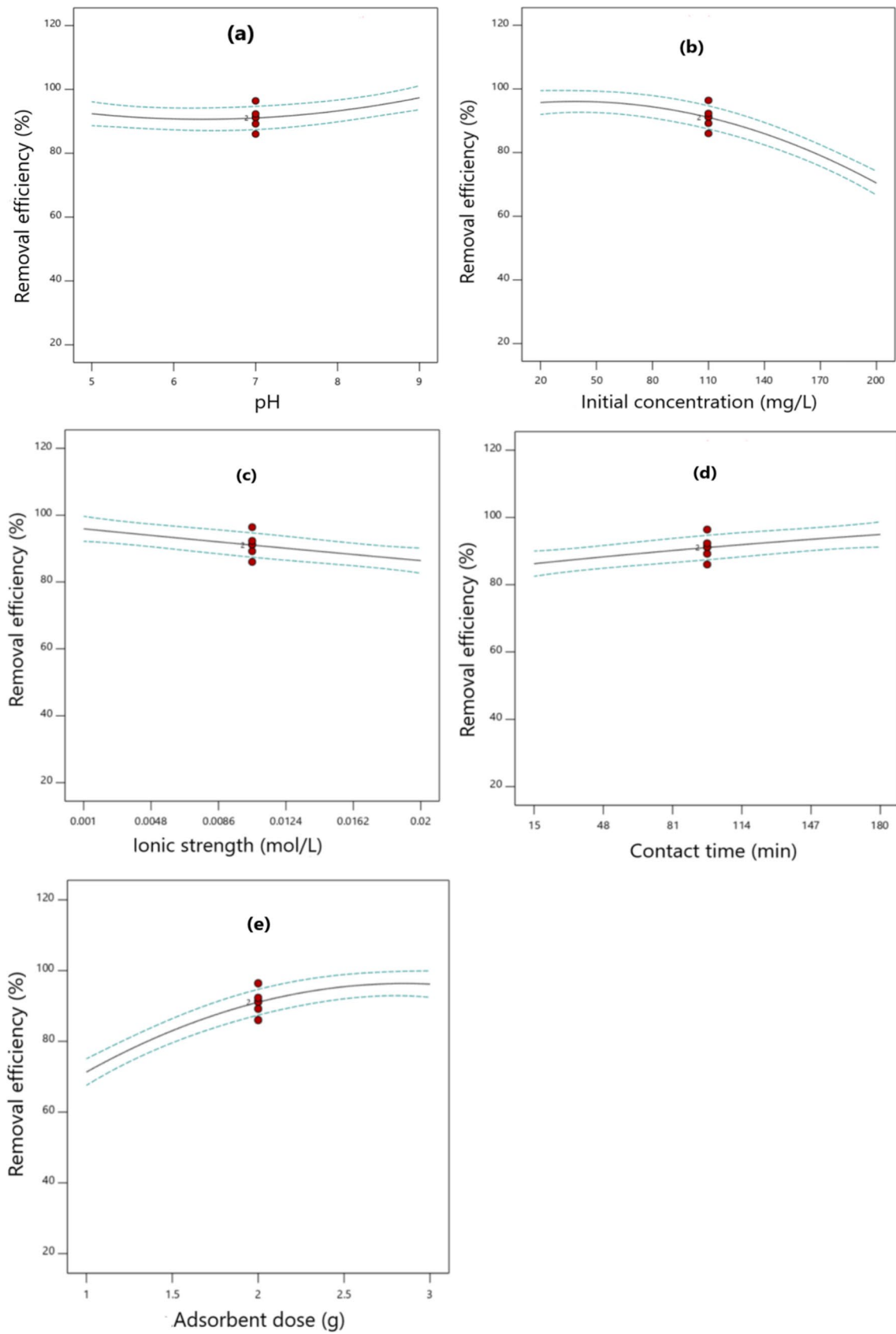
**Fig. 5** Main effect plots of parameters for $Cd^{2+}$ removal efficiency on BSD/RH adsorption process
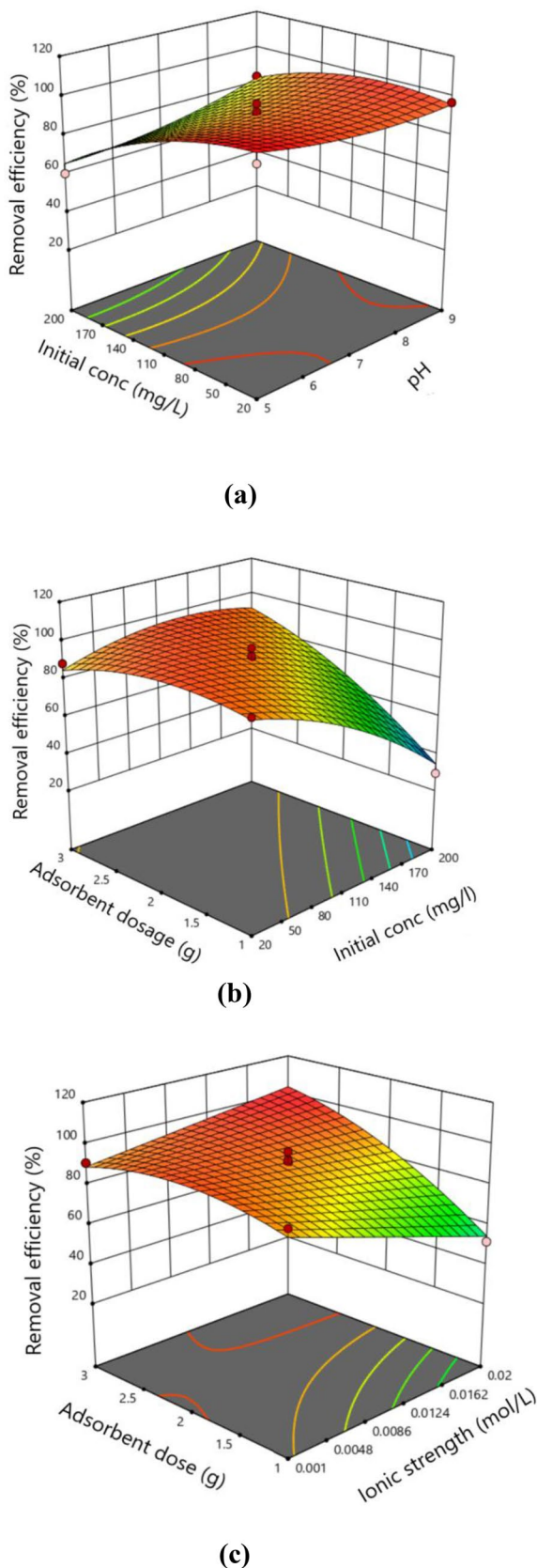
**(a)**



**(b)**



**(c)**

**Fig. 6** The combined effect of **a** initial concentration and pH, **b** adsorbent dose and initial concentration, **c** adsorbent dose and ionic strength on Cd$^{2+}$ % removal efficiency

### 3.4.2 Influence of Initial Cd$^{2+}$ Concentration

The Cd$^{2+}$ percentage removal efficiency appears to decrease with an increase of initial Cd$^{2+}$ concentration. The significant decrease started from 80 to 200 mg/L as shown in Fig. 5b. Because the active sites of the adsorbent are surrounded by more Cd$^{2+}$ in the solution at higher solute concentrations, the adsorbent's equilibrium adsorption capacity improves as the Cd(II) ion concentration rises, improving the adsorption process. Furthermore, as the metal starting concentration rises, the removal % decreases. Because the ratio of the initial number of Cd$^{2+}$ to the accessible active sites of the adsorbent is low at low solute concentrations, the removal efficiency of Cd(II) is higher, and more residual Cd(II) ions remain in the aqueous solution at higher concentrations [50].

### 3.4.3 Ionic Strength Influence

From the plot (Fig. 5c) it can be noticed the decrease in Cd$^{2+}$ percentage removal efficiency as Ionic strength increases. This can be due to an increase in competition between Cd$^{2+}$ and K$^+$ from KNO$_3$ solution over the available adsorption sites on the adsorbent surface. The adsorbed K$^+$ at the adsorption site of the adsorbent, block Cd$^{2+}$ from accessing the adsorption site. As the number of K(I) ions increases the competition between it and Cd(II) becomes more tense leaving more residual Cd(II) ions in the solution un-adsorbed [51]. Also, it can be associated with precipitation of the metal to salt (Cd(NO$_3$)$_2$) as the concentration of NO$_3^-$ increases by increasing background electrolyte (KNO$_3$) in the solution [52].

### 3.4.4 Influence on Contact Time

In the batch adsorption process, contact time is one of the most important elements. The adsorption rate grew rapidly at first, and the ideal removal efficiency was obtained in around 147 min for any initial concentration, as shown in Fig. 5d. The uptake of the Cd(II) ion proceeded in two stages, with the first being quick and the second being gradual. When the number of potential adsorption sites is substantially greater than the number of metal species to be adsorbed, the adsorption process appears to move quickly [53]. The contact time required increased as the amount of metal adsorbed increased. A saturation of adsorption sites on the BS/RH adsorbent can be attributed to the subsequent slow absorption (beyond 147 min from Fig. 5d). After 147 min, there was no significant change in the equilibrium concentration, indicating that the adsorption phase had reached equilibrium.

**Table 5** Experimental and predicted results on a few selected solutions suggested for optimization tests for $Cd^{2+}$ removal by BSD/RH adsorbent

| pH | Initial concentration (mg/L) | Ionic strength (mol/L) | Contact time (min) | Adsorbent dosage (g) | Predicted (%) | Experimental (%) | Adsorption capacity (mg/g) | Desirability |
|---|---|---|---|---|---|---|---|---|
| 9 | 163 | 0.012 | 126 | 2 | 90.56 | 88.97 | 73.8 | 1 |
| 9 | 152 | 0.018 | 143 | 2 | 90.33 | 88.61 | 68.65 | 1 |
| 9 | 160 | 0.01 | 149 | 2 | 90.27 | 87.83 | 72.2 | 1 |

### 3.4.5 Effect of Adsorbent Dosage

Since the contact surface of adsorbent particles became more available, cadmium removal efficiency improved correspondingly with the adsorbent dosage increase, as seen in Fig. 5e. Increased adsorbent dosage results in more active sites for adsorption, making metal ion penetration to the adsorption sites simpler [12]. At a dosage of 2.5 g of adsorbent, 100% removal was observed. Adsorption of any adsorbent dose greater than 20 mg/L resulted in roughly the same uptake. As a result, the utilization of a 2.5 g adsorbent dose may be sufficient to justify the method in terms of cost.

### 3.5 Combined Effect of Operational Parameters on Cadmium % Removal Efficiency

In this study, among the total of ten possible combinations between two operating parameters on effect on $Cd^{2+}$ removal tested by RSM, only three interactions of them were found significant. These combinations were between; initial concentration and adsorbent dosage (BE), contact time and adsorbent dosage (CE), and lastly between pH and initial $Cd^{2+}$ concentration (AB) as discussed above.

Figure 6a shows the 3-dimensional surface plot of the combined effect of pH and initial solute concentration (AB). It can be observed that maximum % Cd(II) removal was obtained in the basic range of 8–9 at a lower initial Cd(II) concentration. Within this condition, the residual $Cd^{2+}$ was insignificant in the supernatant as well as $H^+$ was minimum to out-compete $Cd^{2+}$ over the adsorption sites of the BSD/RH adsorbent. Figure 6b shows the 3-dimensional surface plot of the combined effect between initial concentration and adsorbent dosage (BE). The $Cd^{2+}$ % removal efficiency was maximum at a higher adsorbent dosage of about 2.5 g at a lower initial solute concentration. At this condition, there were enough adsorption sites to be offered by BSD/RH adsorbent materials to accommodate all available $Cd^{2+}$ from the solution i.e. High adsorbent dose enhances complex formation between the metal ions and adsorbent [44]. The combined effect of contact time and adsorbent dose (CE) effect on $Cd^{2+}$ % removal is illustrated in Fig. 6c. Similarly, at this condition, the maximum $Cd^{2+}$ % removal efficiency

was at a higher adsorbent dosage (2 g) at lower ionic strength (0.001–0.0048 mol/L $KNO_3$). At this condition, the competition offered by $K^+$ from $KNO_3$ to $Cd^{2+}$ over available adsorption site were less intense and so the significant $Cd^{2+}$ were able to be adsorbed.

### 3.6 Process Optimization

Process optimization was carried out using RSM with the analysis set at maximum % Cd(II) removal. The influencing parameters were set as follows; pH (in a range, 5–9), initial solute concentration (maximize, 150–200 mg/L), ionic strength (maximize, 0.005–0.02 mol/L), contact time (minimize, 15–180) and adsorbent dosage (minimize, 1–3 g). Optimum adsorption conditions obtained were pH of 9, ionic strength of 0.012 mol/L $KNO_3$, contact time of 126 min, initial concentration 163 mg/L, and adsorbent dose of 2 g for 90.6% Cd(II) removal equivalent to 73.8 mg/g adsorption capacity at the desirability of 1.00 as presented in Table 5. The function's high desirability indicates that it could represent the experimental model and conditions. The experimental Cd(II) removal was 88.9% under these conditions. For the rest of the two optimized conditions, the % removal efficiencies difference between predicted and experimental values were not significant i.e., 90.3% predicted value to 88.6% experimental value and 90.3% predicted to 87.8% of the experimental value (Table 5). The conditions were chosen to maximize $Cd^{2+}$ % removal efficiency at a minimal adsorbent dosage and contact time and maximal Initial $Cd^{2+}$ concentration and ionic strength while pH was left to be at a range. The model proposed many sets of experiments, and the best three were carried out.

### 3.7 Percentage Removal Efficiency of Individual Feedstocks of Rice Husk and Bamboo Sawdust

Using the optimized parameters obtained in Table 5, i.e. pH of 9, solute concentration of 163 mg/L, ionic strength 0.012 M, and contact time of 126 min at an adsorbent dose of 2 g. The Batch experiment studies were run for individual rice husk and bamboo sawdust to compare the removal efficiency of blended biosorbent against the individual adsorbent materials. The $Cd^{2+}$ removal efficiency of 61.4 and 69.7% were obtained for rice husk and bamboo sawdust

respectively. This may confirm synergistic enhancement of the chemical and physical properties of the surface of blended feedstock.

## 4 Conclusion

In this study, optimization of process parameters for Cd(II) ions adsorption into bamboo sawdust/rice husk biosorbent materials from aqueous solution using BBD–RSM was carried out. To correlate the response with the process variables, a quadratic model was developed.

The parameters investigated include; pH, initial $Cd^{2+}$ concentration, ionic strength, contact time, and adsorbent dosage. The analysis of variance showed that both studied parameters were significant on $Cd^{2+}$ removal from the solution, although the most significant parameters were initial $Cd^{2+}$ concentration and adsorbent dosage both with a p value of $< 0.0001$, followed by ionic strength with a p value of 0.0002, then contact time with a p value of 0.0005 and last was pH with a p value of 0.0296.

Applying the predicted optimum conditions of pH (2), ionic strength (0.012 mol/L), contact time (126 min), and adsorbent dose (2 g), Cd(II) removal of 90.6% was obtained. Furthermost; the blended feedstock adsorbent material has been found to have higher % removal efficiency compared to individual feedstocks of rice husk and bamboo sawdust. This observation signposts the potential of utilizing the multi-feedstock sources (mixture) of known biosorbent materials on enhancing the pollutants removal by adsorption on aqueous systems.

## Declarations

**Conflict of interest** The authors declare that they have no known competing financial interests or personal relationships that could have appeared to influence the work reported in this paper.

## References

1. Idrees N, Tabassum B, Abd Allah EF, Hashem A, Sarah R, Hashim M (2018) Groundwater contamination with cadmium concentrations in some west U.P. regions, India. Saudi J Biol Sci 25(7):1365–1368. https://doi.org/10.1016/j.sjbs.2018.07.005

2. Chen D, Wang X, Wang X, Feng K, Su J, Dong J (2020) The mechanism of cadmium sorption by sulphur-modified wheat straw biochar and its application cadmium-contaminated soil. Sci Total Environ 714:136550. https://doi.org/10.1016/j.scitotenv.2020.136550

3. Zhang Y et al (2021) In situ cadmium removal from paddy soils by a reusable remediation device and its health risk assessment in rice. Environ Technol Innov 23:101713. https://doi.org/10.1016/j.eti.2021.101713

4. Jajuli MN, Mohamed N, Mohd Suah FB (2020) Electrochemical removal of cadmium from a sulphate solution using a three-dimensional electrode. Alexandria Eng J 59(6):4237–4245. https://doi.org/10.1016/j.aej.2020.07.027

5. Jayakumar V, Govindaradjane S, Senthil Kumar P, Rajamohan N, Rajasimman M (2021) Sustainable removal of cadmium from contaminated water using green alga—optimization, characterization and modeling studies. Environ Res 199(April):111364. https://doi.org/10.1016/j.envres.2021.111364

6. Madhavan J, Theerthagiri J, Balaji D, Sunitha S (2019) Ultrasound: an overview. Molecules 24:1–18

7. Sun Y, Zhou S, Sun W, Zhu S, Zheng H (2020) Flocculation activity and evaluation of chitosan-based flocculant CMCTS-g-P(AM-CA) for heavy metal removal. Sep Purif Technol 241(February):116737. https://doi.org/10.1016/j.seppur.2020.116737

8. Goyal P, Tiwary CS, Misra SK (2021) Ion exchange based approach for rapid and selective Pb(II) removal using iron oxide decorated metal organic framework hybrid. J Environ Manag 277(May 2020):111469. https://doi.org/10.1016/j.jenvman.2020.111469

9. Rosa MA, Egido JA, Márquez MC (2017) Enhanced electro-chemical removal of arsenic and heavy metals from mine tailings. J Taiwan Inst Chem Eng 78:409–415. https://doi.org/10.1016/j.jtice.2017.06.046

10. Theerthagiri J et al (2021) Application of advanced materials in sonophotocatalytic processes for the remediation of environmental pollutants. J Hazard Mater 412(January):125245. https://doi.org/10.1016/j.jhazmat.2021.125245

11. Kayranli B (2022) Cadmium removal mechanisms from aqueous solution by using recycled lignocelluloses. Alexandria Eng J 61(1):443–457. https://doi.org/10.1016/j.aej.2021.06.036

12. Kwikima MM, Mateso S, Chebude Y (2021) Potentials of agricultural wastes as the ultimate alternative adsorbent for cadmium removal from wastewater. A review. Sci Afr 13:e00934. https://doi.org/10.1016/j.sciaf.2021.e00934

13. Bhatnagar A, Sillanpää M, Witek-Krowiak A (2015) Agricultural waste peels as versatile biomass for water purification—a review. Chem Eng J 270:244–271. https://doi.org/10.1016/j.cej.2015.01.135

14. Varala S, Ravisankar V, Al-Ali M, Pownceby MI, Parthasarathy R, Bhargava SK (2019) Process optimization using response surface methodology for the removal of thorium from aqueous solutions using rice-husk. Chemosphere 237:124488. https://doi.org/10.1016/j.chemosphere.2019.124488

15. Singh R (2020) Recycling of agricultural waste for wastewater treatment. Elsevier, Amsterdam

16. Wei Y, Shen C, Xie J, Bu Q (2020) Study on reaction mechanism of superior bamboo biochar catalyst production by molten alkali carbonates pyrolysis and its application for cellulose hydrolysis. Sci Total Environ 712:136435. https://doi.org/10.1016/j.scitotenv.2019.136435

17. Renu MA, Singh K, Upadhyaya S, Dohare RK (2017) Removal of heavy metals from wastewater using modified agricultural

adsorbents. Mater Today Proc 4(9):10534–10538. https://doi.org/10.1016/j.matpr.2017.06.415

18. Arthi D, Michael Ahitha Jose J, Edinsha Gladis EH, Shajin Shinu PM, Joseph J (2020) Removal of heavy metal ions from water using adsorbents from agro waste materials. Mater Today Proc. https://doi.org/10.1016/j.matpr.2020.08.738

19. Wang Z, Shu X, Zhu H, Xie L, Cheng S, Zhang Y (2020) Characteristics of biochars prepared by co-pyrolysis of sewage sludge and cotton stalk intended for use as soil amendments. Environ Technol (United Kingdom) 41(11):1347–1357. https://doi.org/10.1080/09593330.2018.1534891

20. Gouws SM, Carrier M, Bunt JR, Neomagus HWJP (2021) Co-pyrolysis of coal and raw/torrefied biomass: a review on chemistry, kinetics and implementation. Renew Sustain Energy Rev 135(July 2020):110189. https://doi.org/10.1016/j.rser.2020.110189

21. Gao R et al (2020) Remediation of Pb, Cd, and Cu contaminated soil by co-pyrolysis biochar derived from rape straw and orthophosphate: speciation transformation, risk evaluation and mechanism inquiry. Sci Total Environ 730:139119. https://doi.org/10.1016/j.scitotenv.2020.139119

22. Liu J, Huang L, Xie W, Kuo J, Buyukada M, Evrendilek F (2019) Characterizing and optimizing (co-)pyrolysis as a function of different feedstocks, atmospheres, blend ratios, and heating rates. Bioresour Technol 277(January):104–116. https://doi.org/10.1016/j.biortech.2019.01.003

23. Li Y, Yu H, Liu L, Yu H (2021) Application of co-pyrolysis biochar for the adsorption and immobilization of heavy metals in contaminated environmental substrates. J Hazard Mater 420(February):126655. https://doi.org/10.1016/j.jhazmat.2021.126655

24. Ahmed MJ, Hameed BH (2020) Insight into the co-pyrolysis of different blended feedstocks to biochar for the adsorption of organic and inorganic pollutants: a review. J Clean Prod 265:121762. https://doi.org/10.1016/j.jclepro.2020.121762

25. Zhang J et al (2020) Co-pyrolysis of sewage sludge and rice husk/bamboo sawdust for biochar with high aromaticity and low metal mobility. Environ Res 191(February):110034. https://doi.org/10.1016/j.envres.2020.110034

26. Liu L, Huang L, Huang R, Lin H, Wang D (2021) Immobilization of heavy metals in biochar derived from co-pyrolysis of sewage sludge and calcium sulfate. J Hazard Mater 403(July 2020):123648. https://doi.org/10.1016/j.jhazmat.2020.123648

27. Scaglioni PT, Badiale-Furlong E (2016) Rice husk as an adsorbent: a new analytical approach to determine aflatoxins in milk. Talanta 152:423–431. https://doi.org/10.1016/j.talanta.2016.02.042

28. Nigatu A, Wondie M, Alemu A, Gebeyehu D, Workagegnehu H (2020) Productivity of highland bamboo (*Yushania alpina*) across different plantation niches in West Amhara, Ethiopia. Forest Sci Technol 16(3):116–122. https://doi.org/10.1080/21580103.2020.1791260

29. Mathewos M (2017) Multiple uses of bamboo species and its contribution to forest resource management in Ethiopia. J Resour Dev Manag 32:123–130

30. Abebe TN (2016) Review of Sesame Value Chain in Ethiopia. Int J African asian Stud 19(27):36–47

31. Mallick D, Poddar MK, Mahanta P, Moholkar VS (2018) Discernment of synergism in pyrolysis of biomass blends using thermogravimetric analysis. Bioresour Technol 261:294–305. https://doi.org/10.1016/j.biortech.2018.04.011

32. Qian Y, Zhang J, Wang J (2014) Pressurized pyrolysis of rice husk in an inert gas sweeping fixed-bed reactor with a focus on bio-oil deoxygenation. Bioresour Technol 174:95–102. https://doi.org/10.1016/j.biortech.2014.10.012

33. Xiong S, Zhang S, Wu Q, Guo X, Dong A, Chen C (2014) Investigation on cotton stalk and bamboo sawdust carbonization for

barbecue charcoal preparation. Bioresour Technol 152:86–92. https://doi.org/10.1016/j.biortech.2013.11.005

34. Zhang Y et al (2017) Bio-char characteristics. BioResources 12(3):4652–4669

35. Aktar J (2021) Batch adsorption process in water treatment. Elsevier, Amsterdam

36. Singh B (2018) Rice husk ash. Elsevier, Amsterdam

37. Tolessa A, Woldeyes B, Feleke S (2017) Chemical composition of lowland bamboo (*Oxytenanthera abyssinica*) grown around Asossa Town, Ethiopia. World Sci News 74:141–151

38. Tir M, Moulai-Mostefa N (2008) Optimization of oil removal from oily wastewater by electrocoagulation using response surface method. J Hazard Mater 158(1):107–115. https://doi.org/10.1016/j.jhazmat.2008.01.051

39. Daghrir R, Drogui P, Zaviska F (2013) Effectiveness of a hybrid process combining electro-coagulation and electro-oxidation for the treatment of domestic wastewaters using response surface methodology. J Environ Sci Heal Part A Toxic Hazard Subst Environ Eng 48(3):308–318. https://doi.org/10.1080/10934529.2013.726840

40. Amani-Ghadim AR, Aber S, Olad A, Ashassi-Sorkhabi H (2013) Optimization of electrocoagulation process for removal of an azo dye using response surface methodology and investigation on the occurrence of destructive side reactions. Chem Eng Process Process Intensif 64:68–78. https://doi.org/10.1016/j.cep.2012.10.012

41. Behbahani M, Moghaddam MRA, Arami M (2011) Techno-economical evaluation of fluoride removal by electrocoagulation process: optimization through response surface methodology. Desalination 271(1–3):209–218. https://doi.org/10.1016/j.desal.2010.12.033

42. Box GEP, Behnken DW (1960) Some new three level design for study of quantitative variables Box Behnkee.pdf. Technometrics 2(4):455–475. https://doi.org/10.1080/00401706.1960.10489912

43. Saldaña-Robles A, Guerra-Sánchez R, Maldonado-Rubio MI, Peralta-Hernández JM (2014) Optimization of the operating parameters using RSM for the Fenton oxidation process and adsorption on vegetal carbon of MO solutions. J Ind Eng Chem 20(3):848–857. https://doi.org/10.1016/j.jiec.2013.06.015

44. Olalekan AP, Fakinle BS, Dada AO, Akpor OB, Oribayo O (2019) Optimization of lead adsorption on rice-husk supported zerovalent iron nanoparticles using response surface methodology. Nano Hybrids Compos 25:1–11. https://doi.org/10.4028/www.scientific.net/nhc.25.1

45. Khedmati M, Khodaii A, Haghshenas HF (2017) A study on moisture susceptibility of stone matrix warm mix asphalt. Constr Build Mater 144:42–49. https://doi.org/10.1016/j.conbuildmat.2017.03.121

46. Solgi M, Najib T, Ahmadnejad S, Nasernejad B (2017) Synthesis and characterization of novel activated carbon from Medlar seed for chromium removal: experimental analysis and modeling with artificial neural network and support vector regression. Resour Technol 3(3):236–248. https://doi.org/10.1016/j.reffit.2017.08.003

47. Hill WJ, Hunter WG (1966) A review of response surface methodology: a literature survey. Technometrics 8(4):571–590

48. Nyangi MJ, Chebude Y, Kilulya KF (2020) Fluoride removal efficiencies of Al-EC and Fe-EC reactors: process optimization using Box–Behnken design of the surface response methodology. Appl Water Sci. https://doi.org/10.1007/s13201-020-01297-x

49. Karimifard S, Alavi Moghaddam MR (2018) Application of response surface methodology in physicochemical removal of dyes from wastewater: a critical review. Sci Total Environ 640–641:772–797. https://doi.org/10.1016/j.scitotenv.2018.05.355

50. Gorzin F, Bahri Rasht Abadi MM (2018) Adsorption of Cr(VI) from aqueous solution by adsorbent prepared from paper mill sludge: kinetics and thermodynamics studies. Adsorpt Sci Technol 36(1–2):149–169. https://doi.org/10.1177/0263617416686976

51. Pereira RC et al (2019) The effect of pH and ionic strength on the adsorption of glyphosate onto ferrihydrite. Geochem Trans 20(1):1–14. https://doi.org/10.1186/s12932-019-0063-1

52. Gal IJ, Stojić D, Nikolić RM (1979) Cadmium chloride complexes in anhydrous calcium nitrate-potassium nitrate melts. Inorg Chem 18(5):1378–1381. https://doi.org/10.1021/ic50195a045

53. Panda H, Tiadi N, Mohanty M, Mohanty CR (2017) Studies on adsorption behavior of an industrial waste for removal of chromium from aqueous solution. S Afr J Chem Eng 23:132–138. https://doi.org/10.1016/j.sajce.2017.05.002